OncoTargets and Therapy

Dovepress
Taylor & Francis Group

Open Access Full Text Article

ORIGINAL RESEARCH

Pan-Cancer Analysis of WRN: From Multi-Omics Biomarker Discovery to Therapy-Guiding Functional Evidence

Qing-Qing Yao[1], Yue Qi[2], Pei-Qin Shi[3], Zi-Ye Yang[1], Pengpeng Qu[1,4], Wen-Wen Zhang[4]

[1]Department of Gynecological Oncology, Tianjin Central Hospital of Gynaecology Obstetrics, School of Medicine, Nankai University, Tianjin, People's Republic of China; [2]Department of Obstetrics and Gynecology, Peking University People's Hospital, Beijing, People's Republic of China; [3]Clinical School of Obstetrics and Gynecology Center, Tianjin Medical University, Tianjin, People's Republic of China; [4]Department of Gynecological Oncology, Tianjin Central Hospital of Gynaecology Obstetrics, Tianjin, People's Republic of China

Correspondence: Wen-Wen Zhang, Department of Gynecological Oncology, Tianjin Central Hospital of Gynaecology Obstetrics, Tianjin, People's Republic of China, Email zhangsmell2@hotmail.com; Pengpeng Qu, Department of Gynecological Oncology, Tianjin Central Hospital of Gynaecology Obstetrics, School of Medicine, Nankai University, Tianjin, People's Republic of China, Email qu.pengpeng@hotmail.com

Background: The RecQ DNA helicase family member WRN is an important protein for maintaining genome stability. The concept of attention as a synthetic lethal target for MSI-H tumors has garnered significant attention in recent years. However, the role of WRN in cancer development, diagnosis, and prognosis has not yet been systematically evaluated at the pan-cancer level.

Methods: On the basis of multiple public cancer databases, we employed bioinformatics techniques to systematically assess WRN expression, variation, and interaction pathways across various cancers, along with the impact of WRN expression on immune profiling, drug sensitivity, and treatment, as a diagnostic tool. Additionally, we used three cancer cell lines to evaluate the suppressor function of WRN inactivation.

Results: WRN is highly expressed in rapidly proliferating tissues and is dysregulated in a cancer-specific manner, particularly in tumors with hereditary DNA repair deficiencies and myeloid malignancies. WRN expression and variants are correlated with prognosis and immune activation potential in cancers. In digestive cancer and endometrial cancer with a high proportion of MSI-H tumors, WRN is positively associated with MSI/TMB signatures. Pharmacogenomic analyses revealed significant correlations between WRN expression levels and sensitivity to the DNA synthesis inhibitors PI3K, ALK, and IFG1R and other target agents and immunomodulators. In vitro validation using WRN inhibitors demonstrated potent suppression of malignant phenotypes (proliferation, clonogenicity, migration, invasion) in colorectal, endometrial, and ovarian cancer models.

Conclusion: Our study suggests that WRN plays a role in cancer diagnosis and therapy, especially in cancers characterized by replicative stress or defective DNA damage repair, and that WRN can serve as a potential target for cancer immunotherapy or targeted therapies and as a prognostic marker for certain tumors.

Keywords: WRN, diagnostic marker, tumor target therapy, genomic instability, pan-cancer analysis

Introduction

The ability of cells to maintain and regulate genomic stability is crucial for internal balance, and deficiencies in maintaining genomic stability form the basis of many developmental disorders and human diseases, including cancer and premature aging.[1,2] Unexpected mutations arising during DNA replication, cell division, and cellular repair can cause genomic instability, thereby increasing the rate of spontaneous mutations and lead to the accumulation of genetic alterations that drive tumor development.[3] The genetic composition of cancerous cells varies in terms of the number and type of alterations, resulting in tumor heterogeneity.[4] Variations in genomic stability can influence patient prognosis and treatment outcomes.[5]

The RecQ helicase family participates in DNA damage repair pathways and contributes to maintaining genomic stability.[6] Germline mutations inactivating the Werner syndrome helicase (WRN) underlie the pathogenesis of Werner

https://doi.org/10.2147/OTT.S564441
Received: 1 September 2025
Accepted: 13 January 2026
Published: 29 January 2026

syndrome (WS), an autosomal recessive progeroid disorder characterized by accelerated aging phenotypes and pathognomonic features of genomic instability. Notably, WS patients exhibit dramatically increased cancer incidence alongside premature cardiovascular pathologies, with malignancy and myocardial infarction emerging as predominant causes of mortality—a clinical trajectory that establishes WS as a prototypical model for investigating the intersection between DNA repair deficiency, aging, and age-related disease pathogenesis.[7] Recently, WRN has been shown to induce synthetic lethality in microsatellite instability-high (MSI-H) tumors.[8] Furthermore, there has been an oncological examination of WRN in relation to the BRCA2, p53, and ATM pathways.[9–11] The presence of DNA damage can serve as a biomarker and a potential therapeutic target in the context of cancer immunotherapy.[12]

Despite the extensive discourse surrounding the synthetic lethal potential of WRN in MSI-H cancers, there is a paucity of research addressing the mechanisms underlying WRN expression or activity alterations and their implications in cancer development. The evidence supporting the dual role of WRN activity changes in aging and cancer remains inconclusive.[13] In terms of tumor heterogeneity and complexity, WRN function may vary significantly among different tumors.[14,15]

Based on the aforementioned background and the potential roles of WRN in tumorigenesis, we hypothesized that beyond its established synthetic lethal relationship with MSI-H tumors, WRN may harbor additional therapeutic vulnerabilities. Currently, a comprehensive pan-cancer analysis of WRN remains unavailable. To elucidate WRN's functions in cancer development, investigate its correlations with various molecular features, and identify potential WRN-targeted therapeutic strategies, we employed bioinformatics and cellular phenotyping assays to pursue a pan-cancer perspective. Our systematic investigation examined the associations between WRN expression and tumorigenesis, clinical outcomes, and immunological characteristics across multiple cancer types, thereby providing valuable insights for developing WRN-directed cancer therapeutics.

Methods

Expression and Mutation Analysis

The Human Protein Atlas (https://www.proteinatlas.org/) offers data on WRN mRNA expression in diverse tissues, immunohistochemical assessments of WRN in cancer and normal tissues, and the subcellular location distribution of WRN in different cell lines. We utilized TIMER2.0 (http://timer.cistrome.org/) to investigate the mRNA expression of WRN in various cancer and normal tissues within The Cancer Genome Atlas (TCGA). We used the Sangerbox 3.0 tool to explore the relationships between WRN expression in the TCGA database and clinical features. At the protein level, we explored the differences in abundance and phosphorylation site of WRN proteins in tumor and adjacent tissues via the cProSite module of the CPTAC data portal (https://cptac-data-portal.georgetown.edu/cptacPublic/). We explored the frequency of WRN alterations across cancers via the cbioPortal (https://www.cbioportal.org/) database. CNV and single-nucleotide variant (SNV) percentages, as well as methylation differences across cancers, were obtained from the TCGA database via GSCA (https://bioinfo.life.hust.edu.cn/GSCA/#/).

Prognosis and Survival

Survival analyses were conducted on pan-cancer datasets obtained from The Cancer Genome Atlas (TCGA), Therapeutically Applicable Research to Generate Effective Treatments (TARGET), and the Genotype-Tissue Expression (GTEx) databases via Sangerbox 3.0. The evaluation included overall survival (OS), disease-free survival (DFS), disease-specific survival (DSS), and progression-free survival (PFS). Kaplan–Meier curves for OS were generated via GEPIA2 (http://gepia2.cancer-pku.cn/) for tumor types with log-rank p values < 0.05, with the group cutoff established at the median.

Protein Interaction and Enrichment Analysis

The first 20 interacting proteins and relevant interacting genes were obtained from STRING (https://cn.string-db.org) and GeneMANIA (https://genemania.org), respectively. The top 100 interacting genes were used for three ontologies, GO (biological process (BP), molecular function (MF) and cellular component (CC) terms), and KEGG pathway enrichment

analyses. KEGG pathway enrichment and enrichment GO term maps were plotted at https://www.bioinformatics.com.cn, an online platform for data analysis and visualization. The network of enriched term visualization comes from the Metascape database. A subset of enriched terms has been selected and rendered as a network plot, where terms with a similarity > 0.3 are connected by edges. The network is visualized via Cytoscape, where each node represents an enriched term and is colored first by its cluster ID.

Immune Infiltration and Immunotherapy

We employed the Sangerbox3.0 and TISIDB databases (http://cis.hku.hk/TISIDB) to investigate the relationships between WRN expression and the characteristics of tumor-infiltrating lymphocytes, as well as the correlations among tumor-infiltrating immune cells (TIICs) and tumor stemness. Analysis of the relationships between WRN expression levels and MSI and tumor mutation load (TMB) and graphing were obtained from https://www.bioinformatics.com.cn, with data and codes from the TCGAplot package. The Tumor Immune Syngeneic MOuse database (TISMO, http://TISMO.cistrome.org) was utilized to evaluate the ability of WRN expression in mouse immunotherapy cohorts and tumor cell lines to predict the immunotherapy response. Additionally, the Tumor Immune Single-cell Hub 2 (TISCH2, http://tisch.compbio.cn) was employed to analyze single-cell WRN expression within the tumor microenvironment.

Drug Sensitivity Analysis

Drug sensitivity profiles and corresponding gene expression datasets were acquired from the CellMiner database (https://discover.nci.nih.gov/cellminer/). Pearson correlation analyses were systematically performed to quantify associations between WRN expression levels and drug sensitivity metrics, thereby interrogating potential links between WRN transcriptional activity and therapeutic response to drugs entering clinical trials or approved by the FDA. Statistical analyses and data visualizations were implemented via the R programming environment (version 4.3.1), with specific reliance on the ggplot2 and ggpubr packages for graphical representation and hypothesis testing.

Cell Culture

HCT116 (human colon cancer cell line), A2780/SK-OV-3/OVCAR-3 (human ovarian cancer cell line) and HEC1-B (human endometrial cancer cell line) cells were obtained from the American Type Culture Collection (ATCC, Rockville, MD, USA). The HCT116 and SK-OV-3 cells were cultured with DMEM (Gibco, Shanghai, China) containing 10% FBS (HyClone, Logan, UT, USA) and 1% penicillin/streptomycin (Gibco, Shanghai, China) at 37°C with 5% CO2 and saturated humidity. The A2780 and OVCAR-3 cells were cultured in 1640 and the HEC-1B cells were cultured in MEM with the same supplements.

RNA Extraction and Real-Time Quantitative Polymerase Chain Reaction (RT–qPCR)

Samples of human tumor tissues and paracancerous tissues were collected from the Department of Gynecologic Oncology, Tianjin Central Obstetrics and Gynecology Hospital. The Ethics Committee of the Department of Obstetrics and Gynecology of Tianjin Central Hospital approved this study after informed consent was obtained from all patients or their families. Total RNA was extracted via TRIzol reagent (Invitrogen, Thermo Scientific, USA). Total RNA was reverse transcribed using cDNA reverse transcription reagent (yeasen, Shanghai, China). PCR amplification was performed in a real-time PCR system with 2×SYBR Green qRT–PCR Master Mix (yeasen, Shanghai, China). Analysis of the RT–qPCR data was performed via the ΔΔCt method. All primers were synthesized by Jinweizhi (Tianjin, China) (WRN, forward primer: 5′-GCCACTGATGCTTATGCTGG; reverse primer: 5′-CCCTCCGTGGGTTTTCCAAT; β-actin, forward primer: 5′-GACCTGACAGACTACCTCAT; reverse primer: 5′-AGACAGCACTGTGTTGGCTA).

Drugs

The WRN helicase inhibitor NSC 617145 was purchased from MCE (NJ, USA), prepared as a 5 mM stock solution in DMSO (Solarbio, Beijing, China) and stored at −20 °C in the dark.

CCK-8 Cell Proliferation Assay

Cell proliferation was assessed via a Cell Counting Kit-8 (Beyotime, Nantong, China) according to the manufacturer's protocol. Briefly, cells were seeded in 96-well plates at a density of 4×10^3 cells per well (n = 3 replicates per group) and allowed to adhere overnight in a humidified incubator at 37°C with 5% CO_2. Following overnight incubation, the cells were treated with various concentrations of NSC617145 (0, 1.25, 2.5, or 5 μM). Cell viability was then quantified at 24, 48, and 72 h posttreatment via the CCK-8 assay. The CCK-8 reagent was mixed with culture medium at a 1:10 (v/v) ratio and incubated at 37°C for 1.5 hours. The absorbance values were subsequently measured at 450 nm via a microplate reader (Molecular Devices, LLC, San Jose, CA, USA) for quantitative analysis.

Colony Formation Assay

A colony formation assay was performed by seeding cells in 12-well plates at a density of 200 cells/well (n = 3 biological replicates). Following overnight adherence, the cells were treated with NSC 617145 at various concentrations (0, 1.25, 2.5, or 5 μM) and maintained for 7 days to allow colony formation. The cells were subsequently fixed with 4% paraformaldehyde (PFA) for 30 min at room temperature, followed by three washes with phosphate-buffered saline (PBS). Colonies were then stained with 1% (w/v) crystal violet solution for 10 min, destained with distilled water, and air-dried. Quantification was performed via ImageJ software (v1.53).

Wound Healing Assay

A wound healing assay was performed by seeding cells in 6-well plates (2×10^5 cells/well) and culturing them in serum-free medium until they reached 90–100% confluency. Following overnight incubation, uniform scratches were created via a sterile 200 μL pipette tip. After washing with PBS, fresh serum-free medium containing NSC 617145 (0, 2.5 μM, or 5 μM) was added. Wound closure was monitored at 0 h and 48 h via phase-contrast microscopy, and quantitative analysis was performed via ImageJ.

Transwell Assay

The cells were resuspended in serum-free medium (2×10^5 cells/mL) and starved for 24 h. The cell suspension (100 μL) was added to the Matrigel-coated upper chambers, while 600 μL of complete medium (20% FBS) was added to the lower chambers. After 24 h of incubation (37°C, 5% CO_2), the cells were fixed with 4% paraformaldehyde and stained with 0.1% crystal violet. The cells on the upper membrane surface were removed via cotton swabs. Invaded cells were imaged under a phase-contrast microscope and quantified by counting four random fields per chamber.

Statistical Methods

Statistical analyses were conducted via source-provided analytical tools for publicly available datasets and GraphPad Prism 9 (GraphPad Software, San Diego, CA, USA) for experimental data. The Mann–Whitney *U*-test was used for statistical analysis of the quantitative RT–PCR data. Two-way ANOVA was used in the CCK-8 experiments. One-way ANOVA was used to analyze the colony and wound scratch assays.

Results

Differential Expression Characteristics of WRN Across Cancers

Human Protein Atlas (HPA) data demonstrated greater WRN expression in tissues with greater repopulation and differentiation capacity, such as the lymphohematopoietic and reproductive systems (bone marrow, endometrium, ovary, and breast), than in neural tissues (hypothalamus, midbrain, and amygdala) (Figure 1A) at the mRNA level. The correlation between WRN expression and tumors is heterogeneous across cancers. TIMER database analysis revealed WRN upregulation in 11 cancer types (CHOL, COAD, ESCA, GBM, HNSC, KICH, LIHC, LUAD, LUSC, and STAD) and downregulation in 5 malignancies (BRCA, KIRC, PRAD, THCA, and UCEC) compared with normal tissues (Figure 1B). Combined with data from the TCGA and GTEx databases, differential expression of WRN across carcinomas revealed that additional information revealed significantly higher expression levels in tumor tissues than in

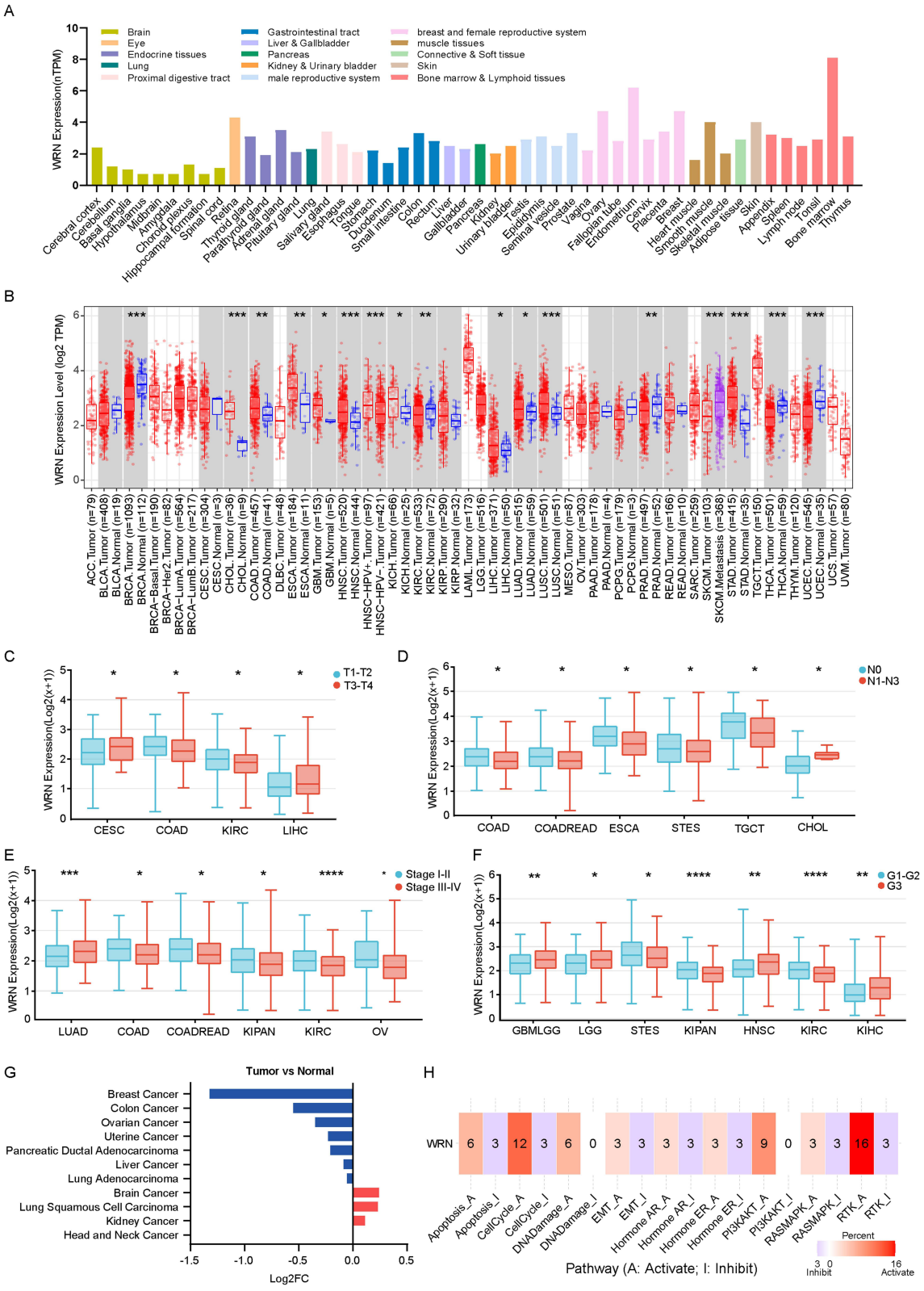

Figure 1 WRN expression and phosphorylation across cancers. (**A**) WRN expression in normal tissues. (**B**) WRN expression across cancers in TIMER. (**C**) Correlation of WRN expression with T stage. (**D**) Correlation of WRN expression with N stage. (**E**) Correlation of WRN expression with clinical stage. (**F**) Correlation of WRN expression with histological grade. (**G**) Differences in WRN protein abundance between tumors and normal tissues. (**H**) Proportion of cancers exhibiting potential WRN expression–pathway activity associations. (* $p < 0.05$, ** $p < 0.01$, *** $p < 0.001$, **** $p < 0.0001$).

https://doi.org/10.2147/OTT.S564441

normal tissues in 7 cancers (LGG, STES, WT, PAAD, TGCT, ALL, and LAML), while WRN expression was reduced in 7 cancers (CESC, LUSC, SKCM, BLCA, OV, UCS, and ACC). LIHC was expressed at lower levels in cancer tissues than in normal tissues, contrary to the results of the TCGA source data alone (Supplementary Figure S1A). Immunohistochemical analysis of the HPA database revealed that WRN expression was significantly lower in tumor tissues than in normal tissues in COAD and PRAD. In contrast, no significant differences in WRN expression levels were observed between tumor and normal tissues in LIHC and UCEC (Supplementary Figure S1B). We confirmed via qRT–PCR that cancer tissues from UCEC patients have lower expression levels of WRN than paracarcinoma tissues do (Supplementary Figure S1C).

We investigated the correlation between WRN expression and pathological features. Analysis of T stage revealed higher WRN expression in advanced-T stages of CESC and LIHC but lower WRN expression in COAD and KIRC (Figure 1C). WRN expression was significantly lower in patients with lymph node metastasis than in those without metastasis in COAD, COADREAD, ESCA, STES, and TGCT, whereas CHOL expression exhibited the opposite trend (Figure 1D). WRN expression was reduced in advanced-stage COAD, COADREAD, KIPAN, KIRC, and OV samples but elevated in LUAD samples (Figure 1E). Furthermore, higher histological grades were associated with increased WRN expression in GBMLGG, LGG, HNSC, and KIHC but decreased WRN expression in STES, KIPAN, and KIRC (Figure 1F).

We also explored the expression of WRN at the protein level. The data from the CPTAC database revealed significantly lower protein abundance in tumors than in control tissues in seven cancers, especially in breast cancer, colon cancer, ovarian and uterine cancer, and significantly greater protein abundance in four cancers than in control tissues, including brain cancer, lung squamous cell carcinoma, kidney cancer, and head and neck cancer (Figure 1G). Among the signaling pathways related to WRN gene expression, RTK is the pathway that is activated in the largest number of cancer types, followed by the cell cycle, PI3K-AKT, apoptosis, and DNA damage repair pathways (Figure 1H).

Molecular Alterations and Epigenetic Modifications of WRN Across Cancers

In terms of the frequency of genetic variants across cancers, endometrial cancer had the highest rate of genetic variants and had the most mutations, followed by hepatobiliary cancer and colorectal cancer. Missense mutations and deep deletions were the most prevalent pan-cancer WRN genetic variants (Figure 2A and Supplementary Figure S1D). Homozygous WRN deletions were detected in 23 of 33 cancer types, with 18 types showing reduced homozygous amplifications (Figure 2B); heterozygous copy number alterations were ubiquitously detected across all analyzed malignancies (Figure 2C). Arm-level deletion is a more prevalent phenomenon in most cancers (Supplementary Figure S1E). With respect to the frequency of SNVs, UCEC presented the highest frequency of mutations, followed by SKCM, STAD and COAD (Figure 2D). Epigenetic modifications revealed increased methylation levels of WRN in cancerous tissues compared with normal tissues in BRCA, COAD, KIRC, KIRP, LIHC, LUSC, PRAD, and UCEC and decreased methylation in HNSC (Figure 2E). Among the nine cancers examined, WRN methylation was negatively correlated with expression in KIRP, LIHC, and PRAD (Supplementary Figure S1F). A phosphorylation heatmap revealed that most of the tumors had relatively high phosphorylation levels in cancer tissues. S1133 was the most common phosphorylation site across cancers, and head and neck cancer had the greatest variety of phosphorylation sites (Figure 2F).

Prognostic Analysis of WRN Across Cancers

Survival data from the TCGA, GTEX, and TARGET databases were analyzed to assess the prognostic significance of WRN expression. Forest plots were constructed for OS, PFS, DFS and DSS across diverse cancer types, and the color represents significance (Figure 3A–D). Elevated WRN expression was significantly correlated with adverse outcomes in multiple cancers: in LGG and KICH, it was associated with poorer OS, PFS, and DFS; in MESO and GBMLGG, it was associated with worse OS and DFS; in LIHC and LAML, it was correlated solely with reduced OS; and in BLCA, it was associated with diminished PFS and DFS. Notably, WRN overexpression had a paradoxical protective effect on specific malignancies. COADREAD patients with elevated WRN expression had improved OS and DFS, whereas KIRC patients had increased PFS and DFS. K–M analysis via the GEPIA platform further validated these findings: high WRN

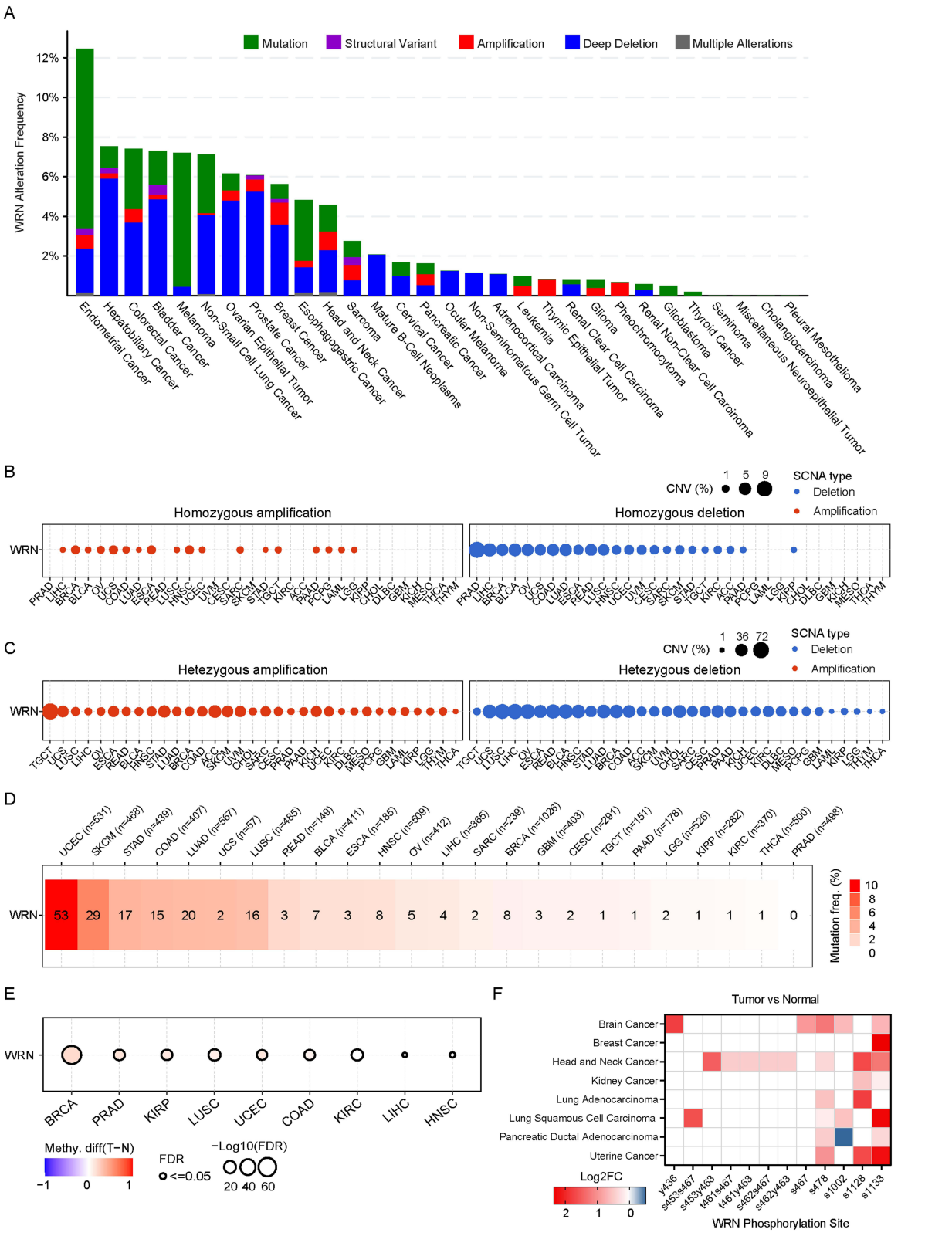

Figure 2 Gene alteration and protein phosphorylation analysis of WRN. (**A**) Frequency of WRN alterations across cancers from the TCGA database via cBioPortal. (**B**) Profile of heterozygous CNVs of WRN across cancers. (**C**) Profile of WRN homozygous CNVs across cancers. (**D**) Pan-cancer profile of SNVs in WRN. (**E**) Methylation differences between tumor and normal samples of WRN across cancers. (**F**) Heatmap of WRN protein phosphorylation differences between tumors and normal tissues.

https://doi.org/10.2147/OTT.S564441

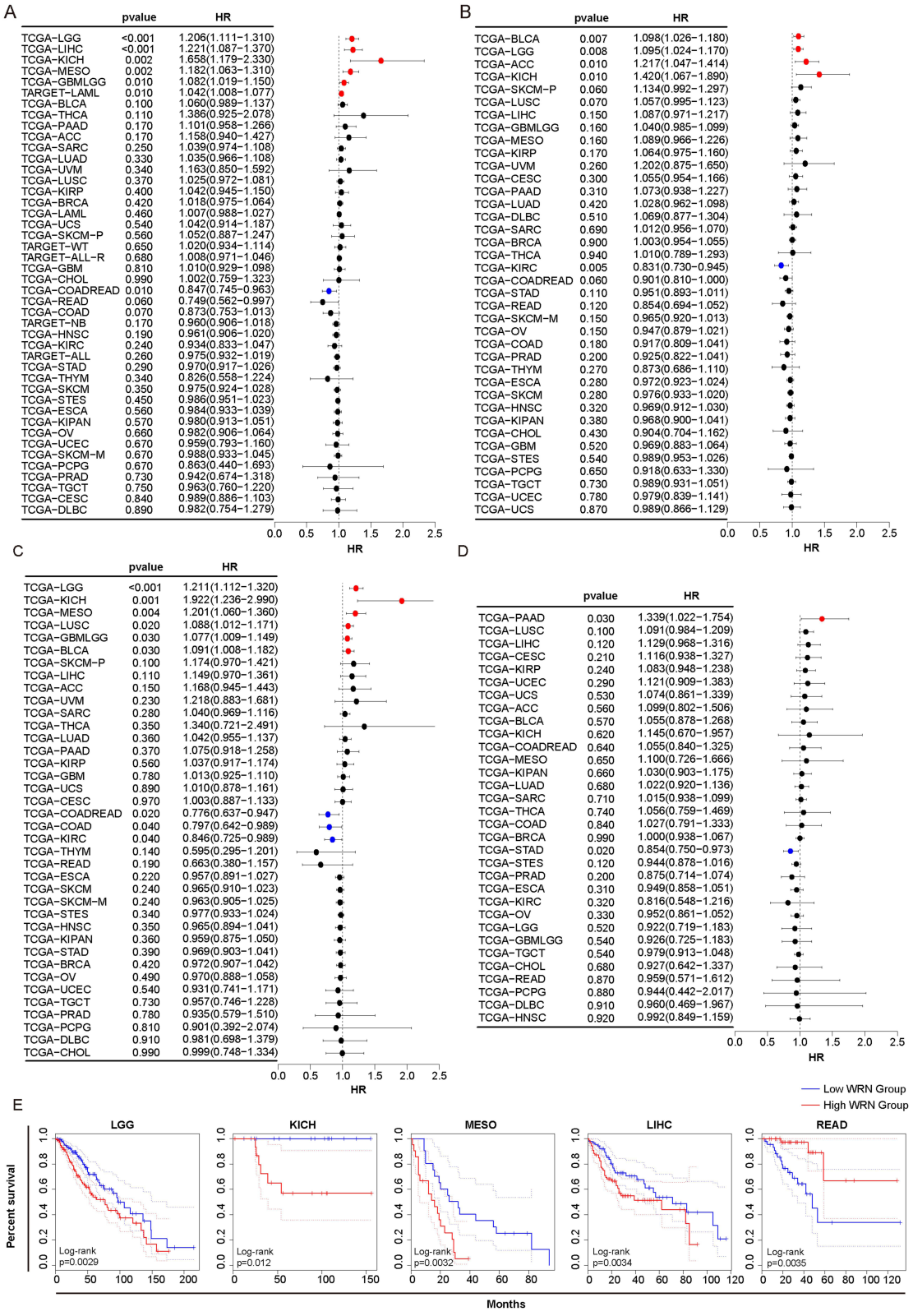

Figure 3 Survival analysis of WRN expression across cancers. (**A**–**D**) Univariate Cox regression of WRN expression and OS, PFS, DFS, and DSS across cancers. (**E**) Kaplan–Meier analysis of the association between WRN expression and OS.

expression significantly worsened OS in LGG, KICH, MESO, and LIHC but conferred superior OS rates in READ (Figure 3E). The relationship between WRN expression and prognosis varies across tumor types and is potentially associated with their distinct pathogenesis and genomic stability status. CNV variants in WRN were risk factors for cancers that had a significant impact on OS, PFS, DSS, and DFI (Figure 4A). In KIRP, UVM, SARC, BRCA, and UCEC, the presence of CNVs in the WRN gene led to a significantly worse outcome than in the wild type (Figure 4B).

WRN Interactome Profiling and Functional Enrichment Analysis

To explore the gene correlations and network of WRN, we integrated multiplatform interactome analyses: physical/pathway-associated gene networks via GeneMANIA (Figure 5A) and protein–protein interaction predictions via STRING (Figure 5B). KEGG pathway and GO functional enrichment analyses were subsequently performed on the top 100 coexpressed genes. KEGG pathway analysis revealed the most significant enrichment in Fanconi anemia, a hereditary hematologic disorder attributed to defective DNA repair mechanisms. Subsequent pathway prioritization demonstrated prominent activation of canonical DNA damage repair pathways, including homologous recombination, mismatch repair, base excision repair, and nonhomologous end joining. Furthermore, the analytical results revealed consequential associations with cellular senescence regulatory networks, platinum drug resistance mechanisms, and cell cycle progression control pathways (Figure 5C). GO enrichment analysis of the interacting genes revealed predominant localization to chromosomal structures and replication forks, with functional enrichment in DNA metabolic processes, including damage response, replication fidelity, and recombination (Figure 5D). To systematically elucidate the functional implications of WRN-associated genes, we conducted comprehensive pathway/process enrichment analysis via Metascape (Figure 5E). This integrative approach incorporated seven ontological systems: the KEGG pathway, the GO biological process, the Reactome gene sets, the canonical pathways, the CORUM, the Wikipathways, and the PANTHER pathway. The resulting top 20 enriched clusters demonstrated predominant associations with DNA repair mechanisms, cellular replication dynamics, and radiation response pathways. To focus on oncologically relevant pathways, we refined the initial set of 100 WRN interactors to a curated list of 52 cancer-associated genes based on protein function

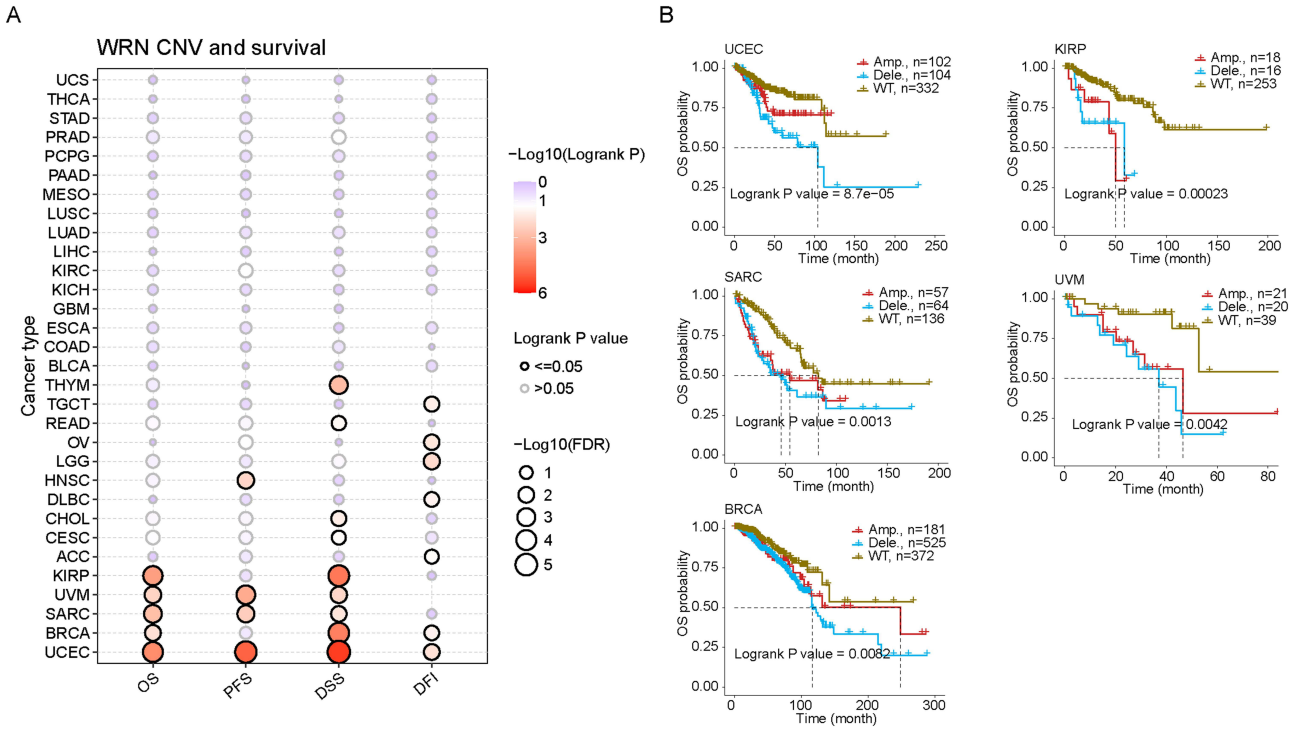

Figure 4 Survival analysis of WRN CNVs across cancers. (**A**) Survival profile of WRN CNV groups across cancers. (**B**) Kaplan–Meier analysis of 5 cancer types with significant correlations between OS and WRN CNVs.

https://doi.org/10.2147/OTT.S564441

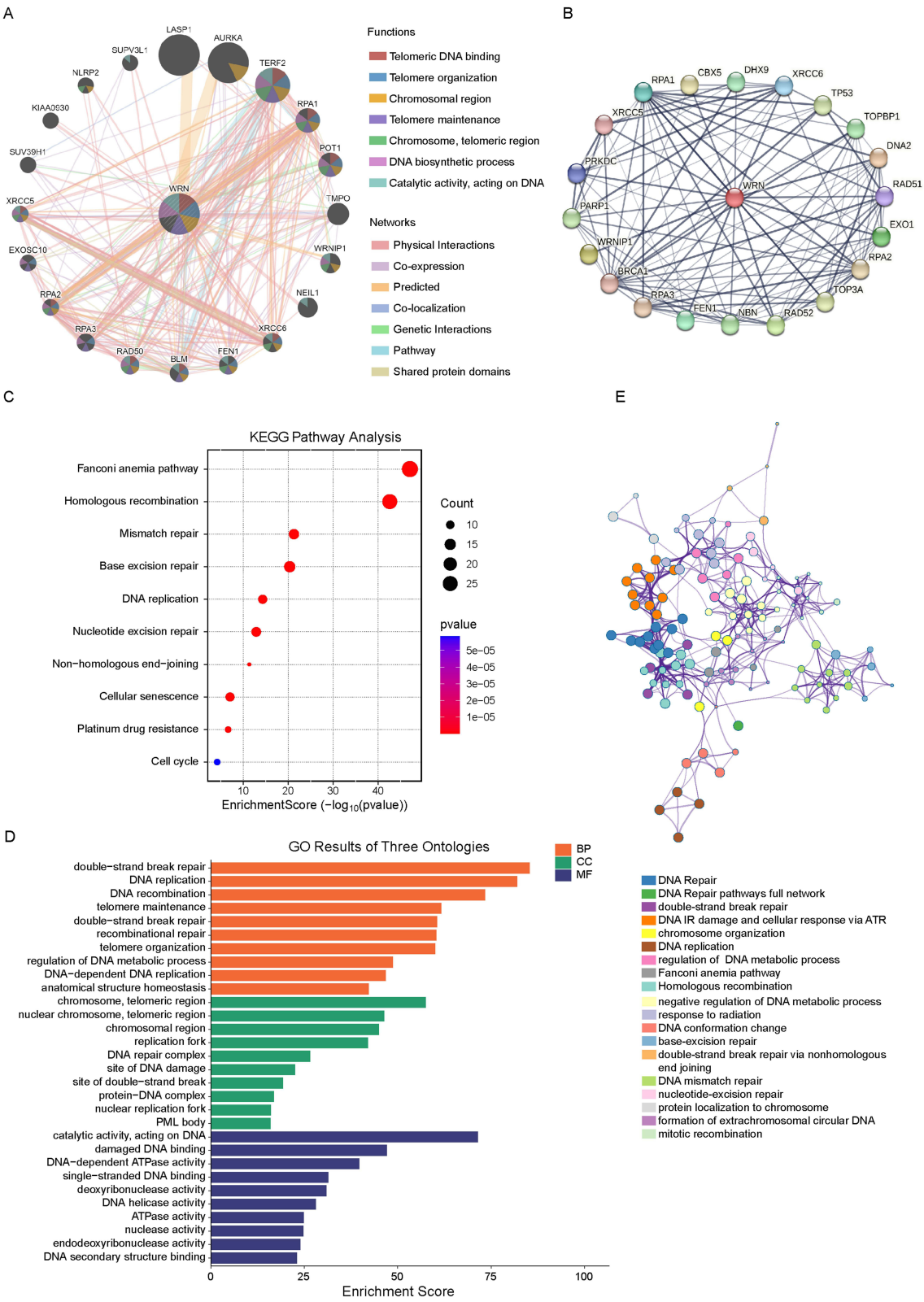

Figure 5 Interaction genes of WRN and functional enrichment analysis. (**A**) Network and functions of genes that interact with WRN. (**B**) Protein–protein interaction (PPI) network of WRN. (**C**) The top 10 KEGG pathways enriched in genes that interact with WRN. (**D**) GO enrichment analysis of genes interacting with WRN. (**E**) Network of enriched pathway terms colored by cluster ID.

annotations for subsequent enrichment analysis. Our analysis revealed that WRN-associated genes converge on core genome stability pathways, such as TP53 regulation, ATM signaling, PID BARD1, and BASC (Supplementary Figure S2A–C). This convergence underscores their combined potential as a cohesive set of targets for therapeutic intervention in WRN-dependent cancers.

Correlation Between WRN Expression and Immune Characteristics

The tumor immune microenvironment actively shapes both disease pathogenesis and therapeutic outcomes, thereby influencing tumor progression and predicting responses to immune-based treatments.[16] To further investigate the interplay between WRN expression and tumor immunogenicity, we systematically analyzed its associations with immune infiltration patterns, the genomic instability markers MSI/TMB, and stemness indices across multiple cancer datasets. Elevated WRN expression was significantly positively correlated with CD4+ T lymphocytes (Act CD4, Tem CD4), Th2 cells and negatively associated with monocyte and macrophage infiltration in most cancer types (Figure 6A and Supplementary Figure S3A). WRN expression was positively associated with UCEC, CESC, COAD, LUSC, OV, READ and STAD but negatively correlated with PRAD, DLBC, and HNSC, suggesting a potential dependency of MSI-high tumor survival on WRN-mediated pathways in most malignancies, with alternative salvage mechanisms possibly operating in minority cancer types (Figure 6B). WRN expression was positively associated with TMB in UCEC, COAD, READ, SKCM, and STAD but inversely correlated with TMB in BLCA and THCA (Figure 6C). WRN expression was significantly positively correlated with tumor stemness scores in TGCTs, STES, LUSC, and HNSC (Figure 6D and Supplementary Figure S3B). WRN expression was strongly negatively correlated with ESTIMATE scores in GBM, UCEC, LAML, SARC, WT and NB (Figure 6E), suggesting that decreased WRN levels may serve as a predictive biomarker for favorable immune infiltration patterns and enhanced therapeutic responsiveness in these malignancies.

Single-Cell-Level Expression of WRN in the TME and Its Relationship with Pathway Activation

We examined single-cell datasets from the TISCH database to elucidate WRN expression in the tumor microenvironment (TME) across cancers. WRN was expressed in malignant, endothelial and monocyte–macrophages (Figure 7A). We analyzed WRN expression in single-cell datasets from multiple cancer types, including HB, AML, PRAD and CRC (Figure 7B, C, Supplementary Figure S4A and B). Single-cell RNA-seq datasets HB_GSE180665 and AML_GSE116256 were used to demonstrate the expression of WRN at the single-cell level and its association with pathway activation in the UMAP plot (Figure 7B and C). WRN had high expression levels in HBs, mainly in malignant cells, and Erypro cells in AML. Moreover, the distribution of WRN expression was found to be correlated with the activation of signaling pathways related to DNA damage repair, apoptosis, the cell cycle, and the inflammatory response in single-cell pathway activation UMAP plots. High expression of WRN was positively correlated with the distribution of DNA repair, E2F target and G2M checkpoint proteins, and low expression of WRN was positively correlated with the activation of P53, apoptosis and the inflammatory response.

Drug Sensitivity Correlations with WRN Expression

Our correlation analysis integrated gene expression profiles and drug *z* scores acquired from the Cell Miner database across 60 cancer cell lines to investigate associations between WRN expression levels and therapeutic susceptibility. Higher *z* scores predict more sensitive cells to drugs. Notably, cells with low WRN expression presented increased sensitivity to cell cycle regulators and DNA metabolism-targeting agents (dinaciclib, actinomycin D, depsipeptide) and targeted therapies against key signaling nodes (PI3K[GSK2126458], ALK[Brigatinib], IGF1R[BMS-536924], ERK1 [Pluripotin], Sp1[Mithramycin A] and FAK[PF-562271] inhibitors) (Figure 8A and Supplementary Figure S5A). WRN-high cell populations exhibited increased susceptibility to immunosuppressive/anti-inflammatory therapeutics (dexamethasone, methylprednisolone, and chelerythrine), DNA synthesis inhibitors (idoxuridine and fludarabine) and topoisomerase inhibitors (Figure 8B and Supplementary Figure S5B). Furthermore, the expression of WRN in cancer immunotherapy was identified through analysis of the TISMO database. The expression of WRN was significantly

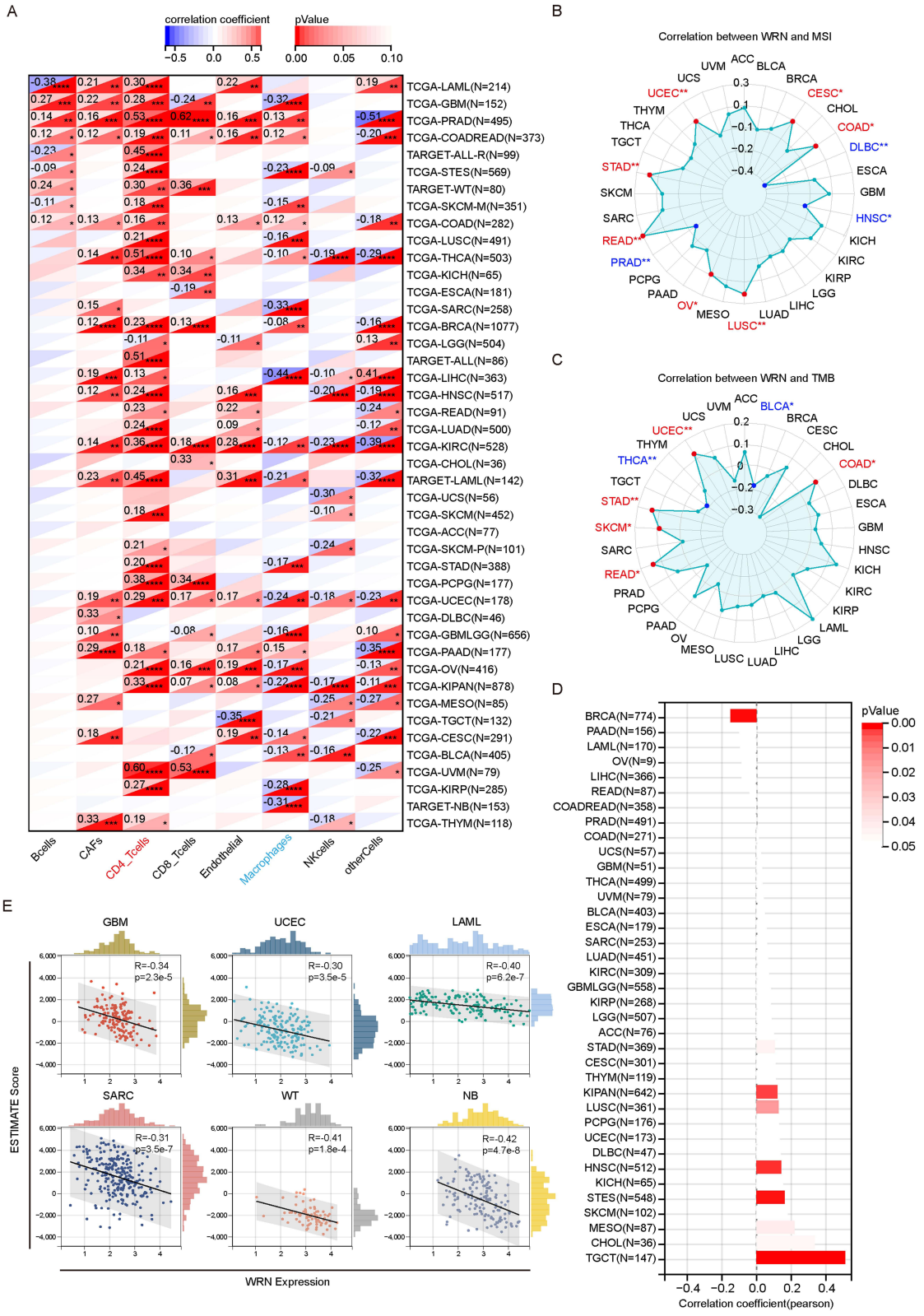

Figure 6 Correlation analysis of WRN expression with immune characteristics across cancers Correlation between WRN expression and (**A**) immune cell infiltration (EPIC algorithms). (**B**) MSI. (**C**) TMB. (**D**) Tumor stemness scores (DNAss). (**E**) ESTIMATE score. (* $p < 0.05$, ** $p < 0.01$, *** $p < 0.001$, **** $p < 0.0001$).

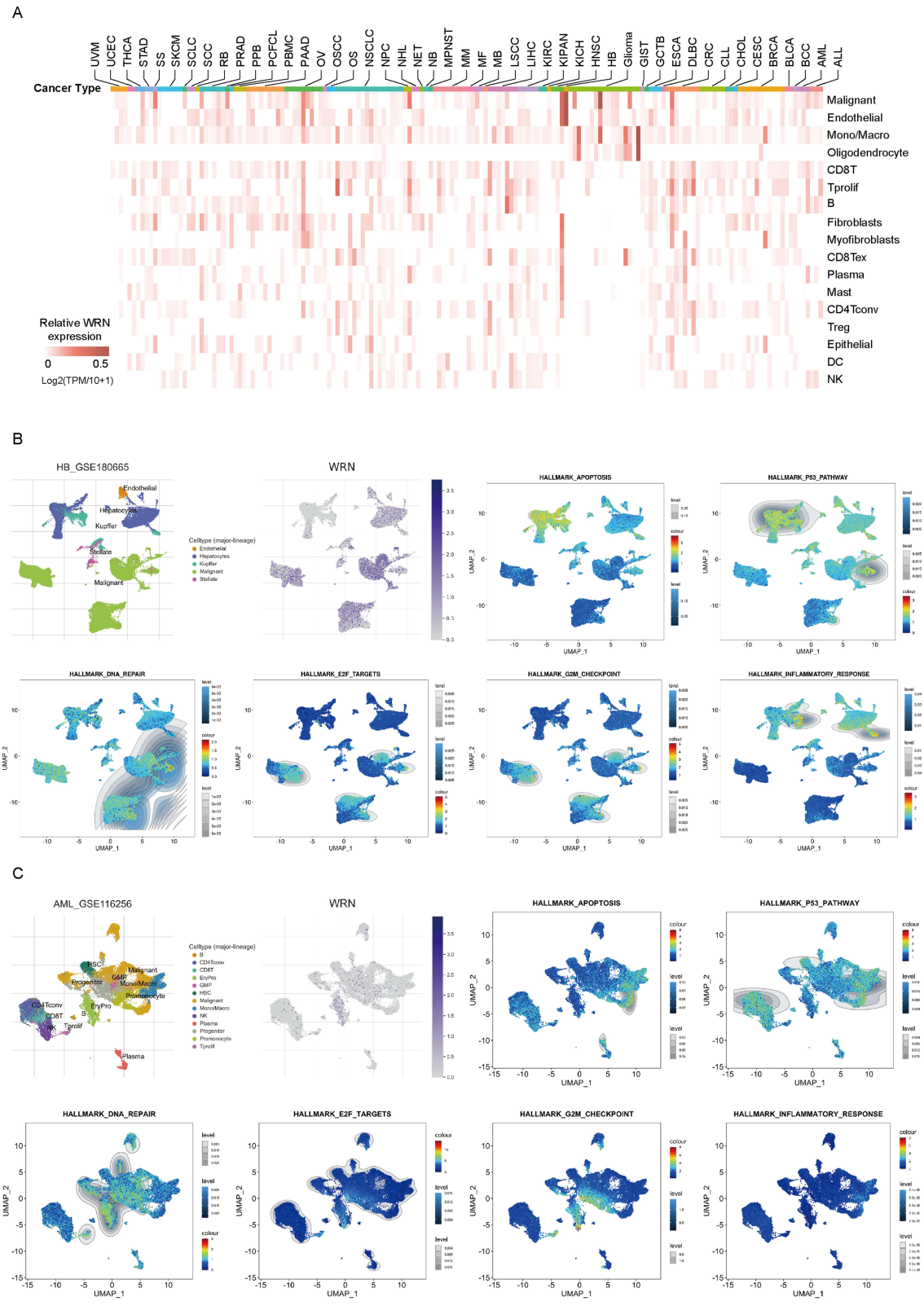

Figure 7 Relationships between WRN expression and (**A**) TME and pathway activation, analyzed at the single-cell level in (**B**) HB and (**C**) AML.

https://doi.org/10.2147/OTT.S564441

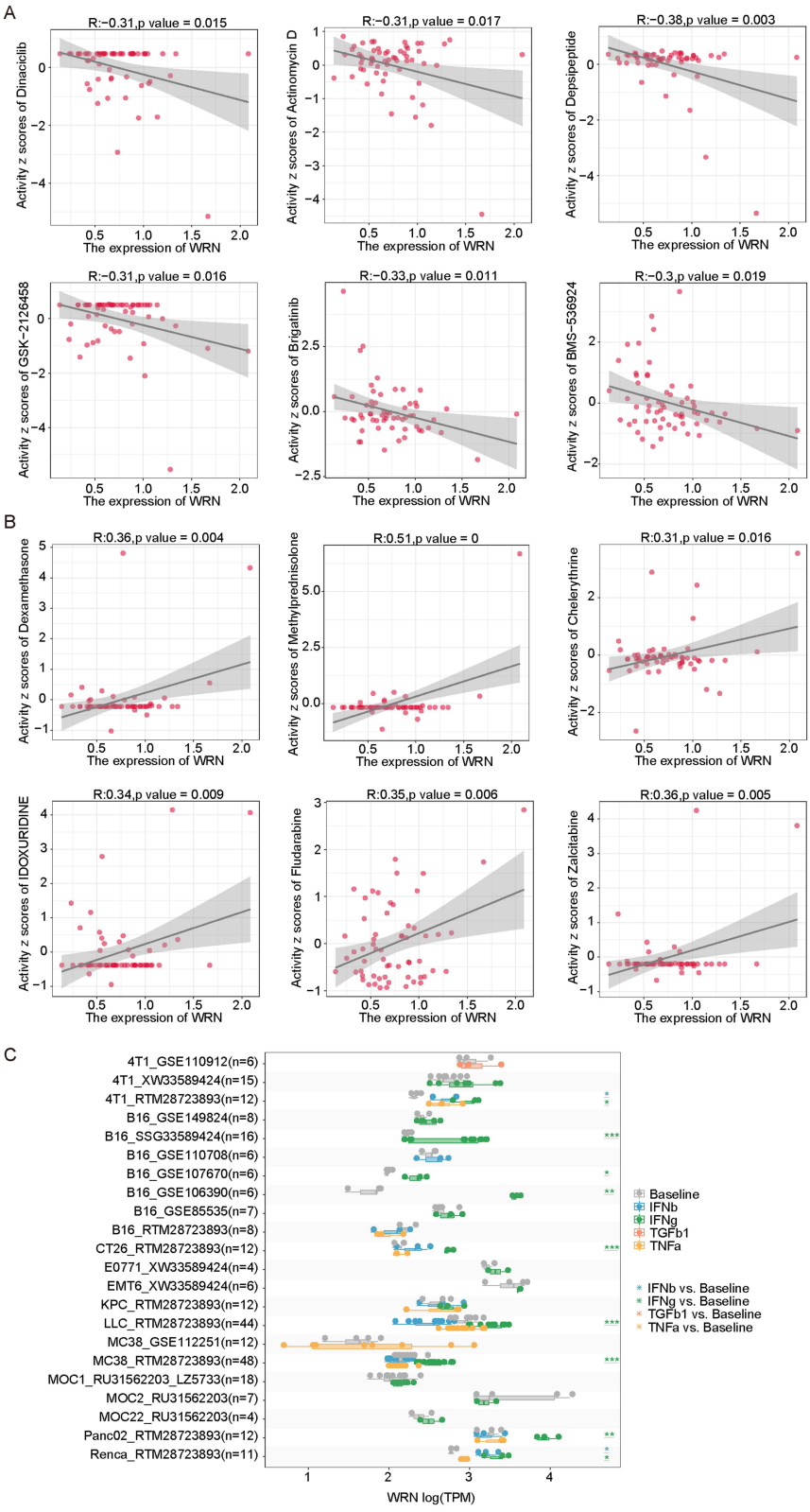

Figure 8 Associations between WRN expression and drug sensitivity. (**A**) WRN expression is negatively correlated with drugs response (z-score) in the CellMiner database. (**B**) WRN expression is positively correlated with drugs response (z-score) in the CellMiner database. (**C**) Relationships between WRN expression and interferon gamma, interferon beta, and TNF alpha treatment in various cell line models from the TISMO database. (* $p < 0.05$, ** $p < 0.01$, *** $p < 0.001$).

increased following the administration of interferon gamma in the majority of the cancer cell lines examined (Figure 8C). Immune checkpoint inhibitor treatment did not significantly affect WRN expression in the majority of in vivo models (Supplementary Figure S6A–C).

WRN Activity Suppression Inhibited the Proliferation and Invasion of Cancer Cells

To systematically evaluate the functional consequences of WRN inhibition, we employed NSC617145, a validated WRN deconjugase inhibitor,[17] in three distinct tumor models: colorectal cancer HCT116 cells, ovarian cancer A2780 cells, and endometrial carcinoma HEC1-B cells. Quantitative CCK-8 proliferation assays revealed significant growth suppression across all the models, with A2780 cells exhibiting increased sensitivity. Both HCT116 and HEC1-B cells exhibited dose-dependent responses (Figure 9A–C). Colony formation capacity, assessed through standardized colony formation assays, revealed parallel attenuation patterns, confirming the anti-proliferative effects observed in the assays (Figure 9D and E). Functional characterization through scratch wound healing assays demonstrated concentration-dependent migratory impairment (Figure 9F and G). Matrigel invasion assays revealed potent suppression of invasive potential, with concentration-dependent reductions in transmigrated cells in all the cell cultures (Figure 9H and I). However, when we assessed the proliferative potential of MSS ovarian cancer cell lines treated with a WRN inhibitor, no significant growth suppression was observed (Supplementary Figure S7A–D).

Discussion

Initially, recognized as the pathogenic gene underlying WS, WRN was characterized primarily as a guardian of replication fork progression and homologous recombination-mediated DNA repair.[18] Particularly noteworthy is the discovery of WRN synthetic lethality in MSI-H cancer, which has sparked substantial interest in exploring its therapeutic potential in MSI-H cancer.[19] However, findings from different studies on various cancers indicate that WRN expression and its modifications play different roles in cancer development and prognosis.[14,15,20,21] In the absence of analysis of WRN across cancers, we explored the function of WRN from multiple bioinformatics databases to determine the role of WRN across cancer types in various aspects of cancer development, prognosis, and treatment.

Our findings on differential WRN expression in normal human tissues are consistent with the results of previous studies in the literature.[22,23] WRN is highly expressed in rapidly dividing cells, suggesting the importance of WRN in cell division activity. Furthermore, it has been demonstrated that loss of WRN increases the sensitivity of tumor cells to radiotherapy through CHK1.[24] Our pan-cancer analysis revealed that WRN expression differed between cancer and paraneoplastic tissues in most cancers. Notably, we found that cancers with a higher proportion of MSI, such as UCEC, PRAD, and CESC, and cancers with a higher proportion of BRCA mutations, such as BRCA and OV, were characterized by lower WRN expression in cancer tissues. Research has demonstrated that the survival of patients with BRCA2-mutated and MSI-H tumors in vivo and in vitro is WRN dependent.[11,19] In addition, our findings, which were verified in UCEC, indicate that WRN expression is lower in cancer tissues than in paraneoplastic tissues. However, WRN expression is significantly higher in cancer tissues in the myeloid hematopoietic system, where the proportion of MSI is low. This evidence indicates that genomic instability may be a dual factor in tumorigenesis and synthetic lethality caused by low WRN expression.

The substantial variation in clinicopathological stage between high and low WRN expression in certain cancer types underscores the notion that the association between WRN expression and tumor progression is contingent on tumor type and environmental factors. S1133 phosphorylation of WRN is dispensable for relocalization in foci but is involved in the interaction with the MRE11 complex.[25] High WRN protein expression had an activating effect on the tumor-promoting RTK and PI3K/AKT pathways, as reported in previous studies.[26,27]

Previous studies have shown that most of the known mutations in WRN in WS result in the degradation of mRNA and premature termination of protein translation or protein destabilization,[28] and we detected a greater frequency of homozygous WRN CNV deletions than homozygous WRN CNV amplifications in most cancers. Deletion of the 8p chromosome segment where WRN is located has a procarcinogenic effect.[29,30]

Our findings indicated that compared with normal tissues, cancerous tissues from BRCA, PRAD, KIPR, and UCEC presented elevated levels of WRN methylation. A study conducted on meningioma patients also revealed that individuals

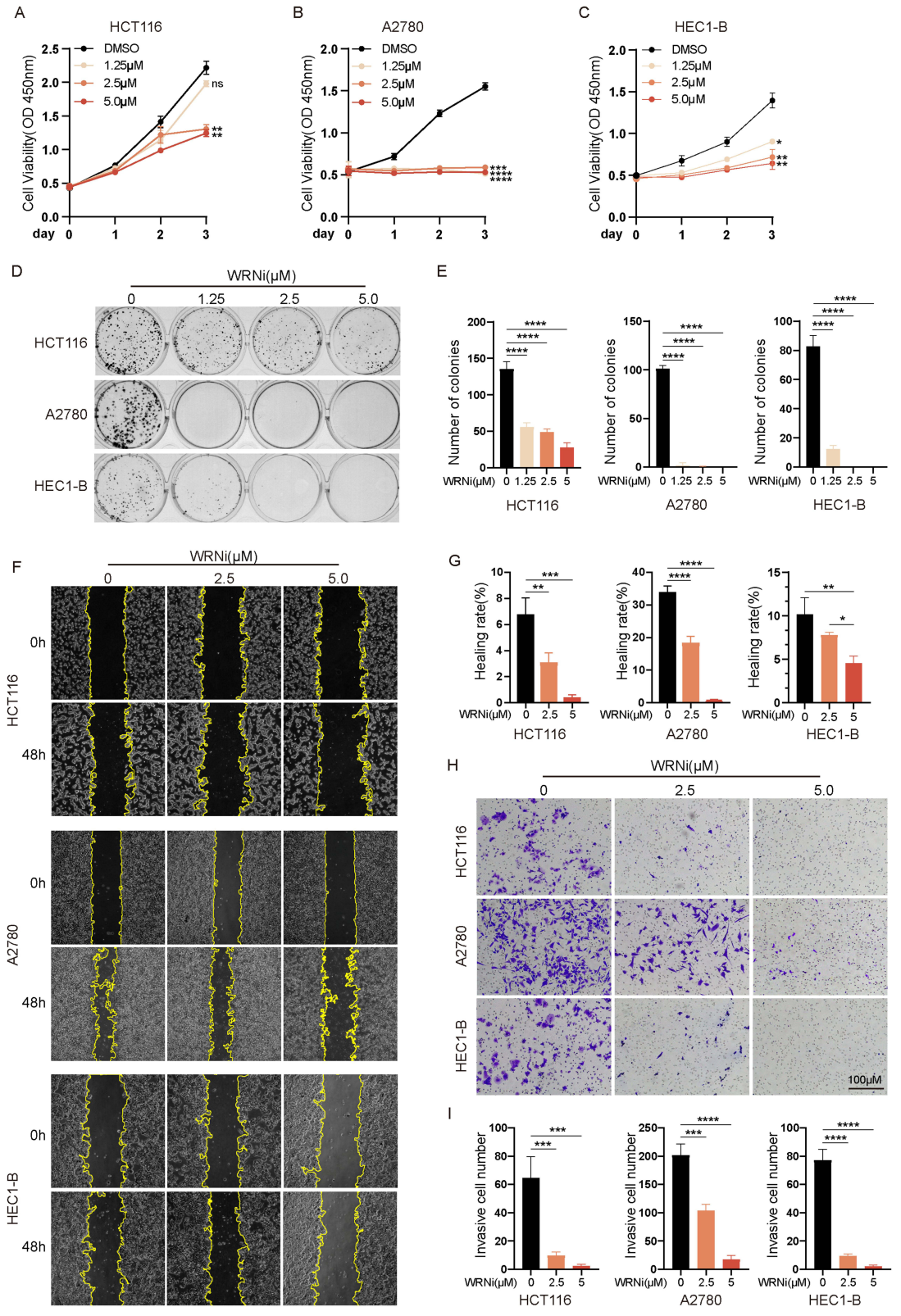

Figure 9 The WRN inhibitor decreased the proliferation and migration ability of three cancer cell lines. (**A**–**C**) Cell viability at different drug concentrations was measured via a CCK8 assay. (**D** and **E**) Cell colony formation abilities under different drug concentrations were assessed via a cloning formation assay. (**F** and **G**) Migration and (**H** and **I**) invasion. (* $p < 0.05$, ** $p < 0.01$, *** $p < 0.001$, **** $p < 0.0001$).

https://doi.org/10.2147/OTT.S564441

diagnosed with this condition presented higher levels of WRN methylation in both tissues and blood samples than did healthy individuals.[31] Furthermore, WRN expression levels were reduced in the group with positive methylation. Additionally, WRN methylation enhances the sensitivity of cervical cancer cells to topoisomerase I inhibitors.[20] Research on colorectal cancer has indicated that WRN expression is not contingent upon WRN promoter methylation status.[21] Lesions with relatively high TMB and CNAs in intestinal metaplasia are considered genomically unstable, with high DNA repair gene WRN, MLH1, and RAD52 promoter hypermethylation.[32] Phosphorylation is a key epigenetic modification that activates the DNA repair function of WRN.[33] Overall, the methylation and phosphorylation of WRN are elevated in cancerous tissues of specific cancer types, thus offering a compelling rationale for further exploration of WRN as a potential target for cancer diagnosis and treatment.

It has been proposed that WRN is an oncogene and that heterozygous deletion of WRN is correlated with a lack of MSI traits, and MSI-high cancers are survival dependent on WRN.[29] Machine learning studies have identified WRN as a prognostic protective factor in OV,[14] and low WRN expression in clinical breast cancer cohorts has also been associated with poor breast cancer prognosis. A sequencing study of a cohort of 234 breast cancer patients revealed that amplification of the 8p12 region where WRN is located (gains in the 8p12 region) was correlated with increased gene expression and independent prediction of chemotherapy sensitivity.[30] Our analysis revealed that specific cancer types were positively correlated with MSI and TMB. These cancer types included UCEC, COAD, STAD, and READ, which presented high proportions of MSI, indicating a potential dependence on WRN expression in these cancers. In the course of our investigation into the prognostic value of WRN, we found that elevated WRN expression in numerous cancers exhibiting low MSI levels predicted decreased survival rates. This observation suggests that the progression of these cancers is contingent on the preservation of genome stability by WRN. A notable example is READ, a cancer type with a substantial MSI proportion, which exhibited enhanced OS in the WRN-high-expression group. This phenomenon may be attributable to synthetic lethal effects. Our findings indicate that the variant groups of WRN CNVs in five cancers presented a poorer prognosis than did the wild-type group.

Genomic instability is a hallmark of both cancer and aging. DNA helicases play a pivotal role in preserving genome stability. DNA damage is the mechanism for synthetic lethality in WRN and MSI-H tumors.[8] DNA damage or repair defects lead to infiltration of the tumor microenvironment by immune cells through the cGAS-STING signaling pathway.[34] However, the relationship between WRN expression and the tumor immune microenvironment has not been thoroughly investigated. Our research revealed a positive correlation between high WRN expression and activated CD4+ T cells and Th2 cells in various cancers. These findings suggest a potential link between WRN expression and humoral immune activation. WRN expression was negatively correlated with monocyte and macrophage numbers. Furthermore, cancers with a high correlation in the ESTIMATE score presented increased immune cell infiltration in tissues with low WRN expression. In summary, we demonstrated a potential correlation between WRN expression and immune function from a bioinformatics perspective.

Notably, our initial exploration of single-cell datasets revealed a negative correlation between WRN expression and apoptosis, the inflammatory response, and p53 pathway activation and a positive correlation with DNA repair, the E2F locus, and G2M checkpoint pathway activation. These findings are consistent with other experimental reports and further elucidate the roles of WRN in cellular activities.[35] Gene drug analysis revealed that low WRN expression was highly sensitive to DNA repair and cell cycle inhibitors, whereas cells with high WRN expression demonstrated increased sensitivity to anti-inflammatory drugs. Werner syndrome protein affects the expression of genes involved in adipogenesis and inflammation.[36] In the in vitro cellular immunotherapy dataset, there was a significant correlation between IFNγ-treated cells and elevated cellular WRN expression.

WRN inhibitors have demonstrated selective cytotoxicity in MSI-H and BRCA2-mutant tumors through interference with DNA replication fork repair mechanisms,[8,11] although evidence suggests that p53 mutations may confer therapeutic resistance.[9] All three cell lines utilized in our in vitro assay are positive for microsatellite instability.[37–39] The assay revealed varying degrees of WRN inhibitor sensitivity, further validating the potential of WRN inhibitors as cancer suppression therapies. However, the limitations of this study include its lack of validation in additional tumor cell lines and its failure to explore further the specific upstream and downstream mechanisms of WRN, as well as immune and

other therapy-related sensitivities. Multi-omics approaches represent a powerful strategy for elucidating complex molecular mechanisms and could help further clarify the functional role of WRN in cancer.[40]

Conclusions

WRN is ubiquitously expressed across human tissues and functions as a critical regulator of DNA repair, with elevated expression and rapid proliferative capacity tissues. WRN not only serves as a prognostic indicator in certain cancers but also emerges as a promising therapeutic target for malignancies with defective DNA damage repair. Furthermore, its dysregulation is associated with immune activation, positioning WRN as a potential biomarker and therapeutic target across multiple cancer types.

Abbreviations

OS, Overall Survival; PFS, Progression Free Survival; DSS, Disease Specific Survival; DFI, Disease Free Interval; AML, Acute myeloid leukemia; ALL, Acute Lymphoblastic Leukemia; ACC, Adrenocortical carcinoma; BLCA, Bladder urothelial carcinoma; LGG, Brain lower-grade glioma; BRCA, Breast invasive carcinoma; CESC, Cervical squamous cell carcinoma and endocervical adenocarcinoma; CHOL, Cholangiocarcinoma; COAD, Colon adenocarcinoma; COADREAD, Colon adenocarcinoma/Rectum adenocarcinoma Esophageal carcinoma; DLBC, Lymphoid Neoplasm Diffuse Large B-cell Lymphoma; ESCA, Esophageal carcinoma; GBM, Glioblastoma multiforme; GBMLGG, Glioma; HNSC, Head and neck squamous cell carcinoma; KICH, Kidney chromophobe; KIPAN, Pankidney cohort (KICH+KIRC +KIRP); KIRC, Kidney renal clear cell carcinoma; KIRP, Kidney renal papillary cell carcinoma; LAML, Acute Myeloid Leukemia; LIHC, Liver hepatocellular carcinoma; LGG, Lower Grade Glioma; LUAD, Lung adenocarcinoma; LUSC, Lung squamous cell carcinoma; DLBC, Lymphoid neoplasm diffuses large B-cell lymphoma; MESO, Mesothelioma; NB, Neuroblastoma; OV, Ovarian serous cystadenocarcinoma; PAAD, Pancreatic adenocarcinoma; PCPG, Pheochromocytoma and paraganglioma; PRCA, Prostate carcinoma; PRAD, Prostate adenocarcinoma; READ, Rectum adenocarcinoma; SARC, Sarcoma; SKCM, Skin cutaneous melanoma; STAD, Stomach adenocarcinoma; STES, Stomach and Esophageal carcinoma; TGCT, Testicular germ cell tumors; THYM, Thymoma; THCA, Thyroid carcinoma; UCS, Uterine carcinosarcoma; UCEC, Uterine corpus endometrial carcinoma; UVM, Uveal melanoma; WT, High-Risk Wilms Tumor.

Data Sharing Statement

The public datasets used in this study are described in the corresponding methods section. Further information can be requested from the corresponding author Wenwen Zhang.

Institutional Review Board Statement

The study was conducted in accordance with the Declaration of Helsinki and approved by the Medical Ethics Committee of Tianjin Central Hospital of Gynecology Obstetrics (Approval number: 2024KY067; Approval date: 2 September 2024).

Informed Consent Statement

Informed consent was obtained from all the subjects involved in the study.

Funding

This study was funded by the Natural Science Foundation of Tianjin Municipality (No. 24JCYBJC01650), the Tianjin Education Commission Scientific Research Project (No. 2023YXZD06), and the Tianjin Key Medical Discipline Construction Project (Grant No. TJYXZDXK-3-029C).

Disclosure

The authors declare that they have no conflicts of interest.

References

1. Negrini S, Gorgoulis VG, Halazonetis TD. Genomic instability--an evolving hallmark of cancer. *Nat Rev Mol Cell Biol*. 2010;11(3):220–228. doi:10.1038/nrm2858
2. Tiwari V, Wilson DM. DNA Damage and Associated DNA Repair Defects in Disease and Premature Aging. *Am J Hum Genet*. 2019;105 (2):237–257. doi:10.1016/j.ajhg.2019.06.005
3. Tubbs A, Nussenzweig A. Endogenous DNA Damage as a Source of Genomic Instability in Cancer. *Cell*. 2017;168(4):644–656. doi:10.1016/j.cell.2017.01.002
4. MacConaill LE, Van Hummelen P, Meyerson M, Hahn WC. Clinical implementation of comprehensive strategies to characterize cancer genomes: opportunities and challenges. *Cancer Discov*. 2011;1(4):297–311. doi:10.1158/2159-8290.CD-11-0110
5. Liu Q, Hu P. Association Analysis of Deep Genomic Features Extracted by Denoising Autoencoders in Breast Cancer. *Cancers*. 2019;11(4):494. doi:10.3390/cancers11040494
6. Croteau DL, Popuri V, Opresko PL, Bohr VA. Human RecQ helicases in DNA repair, recombination, and replication. *Annu Rev Biochem*. 2014;83 (1):519–552. doi:10.1146/annurev-biochem-060713-035428
7. Kudlow BA, Kennedy BK, Monnat RJ. Werner and Hutchinson-Gilford progeria syndromes: mechanistic basis of human progeroid diseases. *Nat Rev Mol Cell Biol*. 2007;8(5):394–404. doi:10.1038/nrm2161
8. van Wietmarschen N, Sridharan S, Nathan WJ, et al. Repeat expansions confer WRN dependence in microsatellite-unstable cancers. *Nature*. 2020;586(7828):292–298. doi:10.1038/s41586-020-2769-8
9. Hao S, Tong J, Jha A, et al. Synthetical lethality of Werner helicase and mismatch repair deficiency is mediated by p53 and PUMA in colon cancer. *Proc Natl Acad Sci U S A*. 2022;119:e2211775119.
10. Ammazzalorso F, Pirzio LM, Bignami M, Franchitto A, Pichierri P. ATR and ATM differently regulate WRN to prevent DSBs at stalled replication forks and promote replication fork recovery. *EMBO J*. 2010;29(18):3156–3169. doi:10.1038/emboj.2010.205
11. Datta A, Biswas K, Sommers JA, et al. WRN helicase safeguards deprotected replication forks in BRCA2-mutated cancer cells. *Nat Commun*. 2021;12(1):6561. doi:10.1038/s41467-021-26811-w
12. Jiang M, Jia K, Wang L, et al. Alterations of DNA damage response pathway: biomarker and therapeutic strategy for cancer immunotherapy. *Acta Pharm Sin B*. 2021;11(10):2983–2994. doi:10.1016/j.apsb.2021.01.003
13. Mukherjee S, Sinha D, Bhattacharya S, Srinivasan K, Abdisalaam S, Asaithamby A. Werner Syndrome Protein and DNA Replication. *Int J Mol Sci*. 2018;19(11):3442. doi:10.3390/ijms19113442
14. Su H, Hou Y, Zhu D, et al. Development of a Prognostic Risk Model Based on Oxidative Stress-related Genes for Platinum-resistant Ovarian Cancer Patients. *Recent Pat Anticancer Drug Discov*. 2025;20(1):89–101. doi:10.2174/0115748928311077240424065832
15. Savva C, Sadiq M, Sheikh O, et al. Werner Syndrome Protein Expression in Breast Cancer. *Clin Breast Cancer*. 2021;21(1):57–73.e7. doi:10.1016/j.clbc.2020.07.013
16. Wang Z-B, Zhang X, Fang C, et al. Immunotherapy and the ovarian cancer microenvironment: exploring potential strategies for enhanced treatment efficacy. *Immunology*. 2024;173(1):14–32. doi:10.1111/imm.13793
17. Aggarwal M, Banerjee T, Sommers JA, et al. Werner syndrome helicase has a critical role in DNA damage responses in the absence of a functional fanconi anemia pathway. *Cancer Res*. 2013;73(17):5497–5507. doi:10.1158/0008-5472.CAN-12-2975
18. Shin S, Hyun K, Lee J, et al. Werner syndrome protein works as a dimer for unwinding and replication fork regression. *Nucleic Acids Res*. 2023;51 (1):337–348. doi:10.1093/nar/gkac1200
19. Ferretti S, Hamon J, de Kanter R, et al. Discovery of WRN inhibitor HRO761 with synthetic lethality in MSI cancers. *Nature*. 2024;629 (8011):443–449. doi:10.1038/s41586-024-07350-y
20. Masuda K, Banno K, Yanokura M, et al. Association of epigenetic inactivation of the WRN gene with anticancer drug sensitivity in cervical cancer cells. *Oncol Rep*. 2012;28(4):1146–1152. doi:10.3892/or.2012.1912
21. Bosch LJW, Luo Y, Lao VV, et al. WRN Promoter CpG Island Hypermethylation Does Not Predict More Favorable Outcomes for Patients with Metastatic Colorectal Cancer Treated with Irinotecan-Based Therapy. *Clin Cancer Res*. 2016;22(18):4612–4622. doi:10.1158/1078-0432.CCR-15-2703
22. Kawabe T, Tsuyama N, Kitao S, et al. Differential regulation of human RecQ family helicases in cell transformation and cell cycle. *Oncogene*. 2000;19(41):4764–4772. doi:10.1038/sj.onc.1203841
23. Polosak J, Kurylowicz A, Roszkowska-Gancarz M, Owczarz M, Puzianowska-Kuznicka M. Aging is accompanied by a progressive decrease of expression of the WRN gene in human blood mononuclear cells. *J Gerontol a Biol Sci Med Sci*. 2011;66(1):19–25. doi:10.1093/gerona/glq162
24. Gupta P, Saha B, Chattopadhyay S, Patro BS. Pharmacological targeting of differential DNA repair, radio-sensitizes WRN-deficient cancer cells in vitro and in vivo. *Biochem Pharmacol*. 2021;186:114450. doi:10.1016/j.bcp.2021.114450
25. Palermo V, Rinalducci S, Sanchez M, et al. CDK1 phosphorylates WRN at collapsed replication forks. *Nat Commun*. 2016;7(1):12880. doi:10.1038/ncomms12880
26. Lutomska A, Lebedev A, Scharffetter-Kochanek K, Iben S. The transcriptional response to distinct growth factors is impaired in Werner syndrome cells. *Exp Gerontol*. 2008;43(9):820–826. doi:10.1016/j.exger.2008.06.007
27. Tu J, Wan C, Zhang F, et al. Genetic correction of Werner syndrome gene reveals impaired pro-angiogenic function and HGF insufficiency in mesenchymal stem cells. *Aging Cell*. 2020;19(5):e13116. doi:10.1111/acel.13116
28. Yokote K, Chanprasert S, Lee L, et al. WRN Mutation Update: mutation Spectrum, Patient Registries, and Translational Prospects. *Hum Mutat*. 2017;38(1):7–15. doi:10.1002/humu.23128
29. Shih J, Sarmashghi S, Zhakula-Kostadinova N, et al. Cancer aneuploidies are shaped primarily by effects on tumour fitness. *Nature*. 2023;619 (7971):793–800. doi:10.1038/s41586-023-06266-3
30. Moelans CB, van Maldegem CMG, van der Wall E, van Diest PJ. Copy number changes at 8p11-12 predict adverse clinical outcome and chemo- and radiotherapy response in breast cancer. *Oncotarget*. 2018;9(24):17078–17092. doi:10.18632/oncotarget.24904
31. Li P, Hao S, Bi Z, Zhang J, Wu Z, Ren X. Methylation of Werner syndrome protein is associated with the occurrence and development of invasive meningioma via the regulation of Myc and p53 expression. *Exp Ther Med*. 2015;10(2):498–502. doi:10.3892/etm.2015.2519

32. Krishnan V, Lim DXE, Hoang PM, et al. DNA damage signalling as an anti-cancer barrier in gastric intestinal metaplasia. *Gut*. 2020;69 (10):1738–1749. doi:10.1136/gutjnl-2019-319002
33. Palermo V, Malacaria E, Semproni M, et al. Switch-like phosphorylation of WRN integrates end-resection with RAD51 metabolism at collapsed replication forks. *Nucleic Acids Res*. 2024;52(20):12334–12350. doi:10.1093/nar/gkae807
34. Nihira NT, Kudo R, Ohta T. Inflammation and tumor immune escape in response to DNA damage. *Semin Cancer Biol*. 2025;110:36–45. doi:10.1016/j.semcancer.2025.02.005
35. Sui Q, Zhou Y, Li M, et al. Design, synthesis, and structure-activity relationship studies of triazolo-pyrimidine derivatives as WRN inhibitors for the treatment of MSI tumors. *Eur J Med Chem*. 2025;282:117039. doi:10.1016/j.ejmech.2024.117039
36. Turaga RVN, Paquet ER, Sild M, et al. The Werner syndrome protein affects the expression of genes involved in adipogenesis and inflammation in addition to cell cycle and DNA damage responses. *Cell Cycle*. 2009;8(13):2080–2092. doi:10.4161/cc.8.13.8925
37. Berg KCG, Eide PW, Eilertsen IA, et al. Multi-omics of 34 colorectal cancer cell lines - a resource for biomedical studies. *Mol Cancer*. 2017;16 (1):116. doi:10.1186/s12943-017-0691-y
38. Ghandi M, Huang FW, Jané-Valbuena J, et al. Next-generation characterization of the Cancer Cell Line Encyclopedia. *Nature*. 2019;569 (7757):503–508. doi:10.1038/s41586-019-1186-3
39. Gorringe KL, Chin S-F, Pharoah P, et al. Evidence that both genetic instability and selection contribute to the accumulation of chromosome alterations in cancer. *Carcinogenesis*. 2005;26(5):923–930. doi:10.1093/carcin/bgi032
40. Li F, Tian J, Zhang L, He H, Song D. A multi-omics approach to reveal critical mechanisms of activator protein 1 (AP-1). *Biomed Pharmacother*. 2024;178:117225. doi:10.1016/j.biopha.2024.117225